IEEE Photonics Journal
An IEEE Photonics Society Publication

Open Access

Group Delay Dispersion Measurement From a Spectral Interferogram Based on the Cubic Phase Function

Volume 6, Number 6, December 2014

Chongxiang Zeng
Hongxia Zhang
Dagong Jia
Tiegen Liu
Yimo Zhang

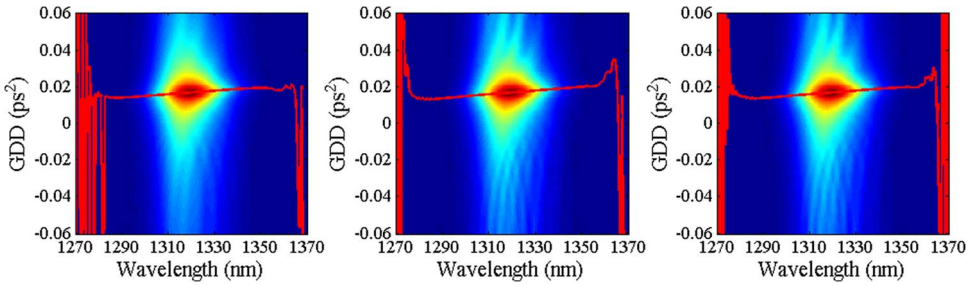

DOI: 10.1109/JPHOT.2014.2366117
1943-0655

Group Delay Dispersion Measurement From a Spectral Interferogram Based on the Cubic Phase Function

Chongxiang Zeng,[1,2] Hongxia Zhang,[1,2] Dagong Jia,[1,2] Tiegen Liu,[1,2] and Yimo Zhang[1,2]

[1]College of Precision Instrument and Optoelectronics Engineering, Tianjin University, Tianjin 300072, China
[2]Key Laboratory of Optoelectronics Information Technical Science, EMC, Tianjin 300072, China

DOI: 10.1109/JPHOT.2014.2366117

Manuscript received September 18, 2014; revised October 17, 2014; accepted October 20, 2014. Date of publication October 31, 2014; date of current version November 13, 2014. This work was supported in part by the National Basic Research Program of China (973 Program) under Grant 2010CB327806 and in part by the National Natural Science Foundation of China (NSFC) under Grant 61205085. Corresponding author: H. Zhang (e-mail: hxzhang@tju.edu.cn).

Abstract: A novel group delay dispersion (GDD) measurement from a spectral interferogram is presented. Based on the cubic phase function (CPF) of the interference term, the GDD can be directly read from the ridge of CPF without phase retrieval and numerical differentiation operation. The proposed method is applied to measure the GDD and chromatic dispersion difference (CDD) of a polarization-maintaining fiber. The experimental results are unambiguous and insensitive to the filter choice of interference term calculation. GDD measurement can reach a resolution of 1 fs^2, with a processing time of 25 s for 1001 wavelength points, and CDD measuring deviation is less than 0.5 $fs/(km \cdot nm)$ around the center wavelength. The method is expected to be suitable for processing all spectral interferograms with polynomial phases.

Index Terms: Metrology, optical properties of photonic materials, fiber optics systems, coherent effects.

1. Introduction

Chromatic dispersion of optical fibers and photonic devices is an important characteristic in optical transmission systems [1], distributed fiber-optic sensors [2], and characterization of ultrashort optical pulses [3], [4]. Spectral interferometry [5]–[8] based on the use of broadband source in combination with a standard Michelson or a Mach-Zehnder interferometer is considered as an effective tool to evaluate the dispersion features of transparent materials. In spectral interferometry, interference fringes are recorded by an optical spectrum analyzer (OSA), with a period inversely proportional to the optical path difference (OPD) between the two beams. The dispersion features are loaded on the spectral phase, and can be resolved from one spectral interferogram.

Prevalent methods measure the group delay dispersion (GDD) by taking a second-order differentiation of the relative phase with respect to the optical angular frequency [6], [7]. For regular dispersion materials, the numerical errors caused by straightforward numerical differentiation can be suppressed by a previous polynomial curve fitting to the relative phase

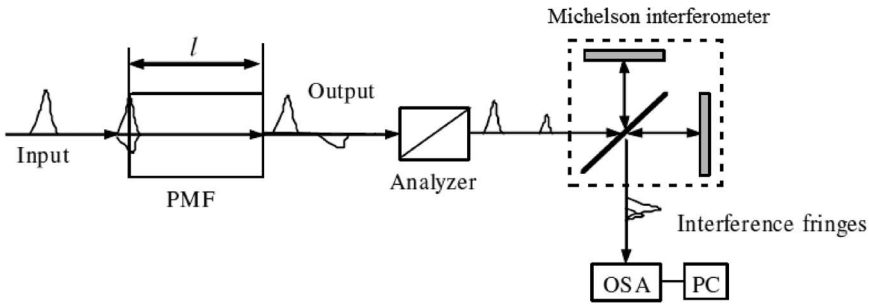

Fig. 1. Schematic of spectral interferometry for GDD measurement.

[6]–[8]. However, the phase is still prone to noise, which is vulnerable to the parameters in the phase retrieval algorithms, such as the filter width in the Fourier-transform (FT) technique [9], the window width in the windowed Fourier-transform (WFT) technique [10] and the wavelet parameters in the wavelet-transform (WT) technique [11]. Consequently, the quadratic and higher-order coefficients of the fitting polynomial, which are proportional to the GDD, are also vulnerable. Deng *et al.* introduced a group delay (GD) measurement technique from the ridge of the Gabor WT [12], but an additional differentiation is necessary to calculate the GDD. The results were proved to be sensitive to the shaping factor of the Gabor wavelet [13].

In this paper, a GDD measurement method to process spectral interferogram without phase retrieval and differentiation operation is introduced for the first time. This data processing method is based on calculating the cubic phase function (CPF) of the interference term. The method is applied to measure the differential GDD between the two polarization modes in polarization maintaining fiber (PMF). The chromatic dispersion difference (CDD) of PMF can be further determined from the GDD. The feasibility of the method was confirmed in processing experimental data of a PMF.

2. Theory of GDD Measurement

Generally, PMF can be regarded as a fiber supporting two polarization eigenmodes. Our measurement principle is based on the interference of the two polarization modes. Consider a schematic diagram of spectral interferometry shown as Fig. 1, linear polarized broadband light is coupled into a PMF under test. If polarization coupling occurs at the input of the PMF, two modes will be both excited at the input of the PMF and propagate through the fiber with different group velocities.

An analyzer is placed at the output of the PMF to make sure that the two light beams can be projected to a same polarization direction and interfere with each other. The interferogram is detected with an OSA. A tandem Michelson interferometer between the analyzer and the OSA is configured to compensate the OPD produced in the PMF. Theoretically, the output spectral interferogram recorded by OSA is [14]

$$I_{out}(\omega) = I_0(\omega) + h \cdot I_0(\omega) + \sqrt{h} \cdot I_0(\omega) \cdot \exp(i\varphi(\omega)) + \sqrt{h} \cdot I_0(\omega) \cdot \exp(-i\varphi(\omega)) \tag{1}$$

where ω is the optical angular frequency; h is wavelength-independent polarization coupling parameter; $I_0(\omega)$ and $h \cdot I_0(\omega)$ are spectral intensity of the two eigenmodes in PMF, respectively; and $\varphi(\omega)$ is the relative phase which contains the entire dispersive properties of PMF. The relative phase can be expressed as [14]

$$\varphi(\omega) = \Delta\beta(\omega) \cdot l - \frac{\Delta d}{c} \cdot \omega \tag{2}$$

where $\Delta\beta(\omega)$ is the differential propagation constant of the PMF, defined as the propagation constant difference of the two eigenmodes, l is the fiber length, Δd is the OPD between the two arms of Michelson interferometer, and c is the velocity of light in vacuum. As the Michelson interferometer is non-dispersive, the GDD of PMF can be obtained by taking a second-order differentiation of (2), calculated as $GDD(\omega) = d^2\varphi(\omega)/d\omega^2$.

The relative phase $\varphi(\omega)$ can be retrieved from the interferogram via FT technique [9]. Firstly, interferogram is converted from frequency domain to time domain by calculating the Fourier transform of the interferogram. The interferogram in time domain is composed of three peaks, that the non-interference term $I_0(\omega) + h \cdot I_0(\omega)$ gives a peak centered at $t = 0$, while the two interference terms $\sqrt{h} \cdot I_0(\omega) \cdot \exp(i\varphi(\omega))$ and $\sqrt{h} \cdot I_0(\omega) \cdot \exp(-i\varphi(\omega))$ give two peaks shifted to $t = \Delta t_{PMF} - \Delta d/c$ (Δt_{PMF} is the differential GD between the two modes in PMF) and $t = \Delta d/c - \Delta t_{PMF}$, respectively. Numerically, one of the two shifted peaks can be filtered and transformed back into the frequency domain. Thus, one of the two interference terms is obtained. The relative phase can then be calculated as the argument of obtained interference term.

A third-order polynomial curve fitting is applied to the relative phase [14], and then the GDD can be obtained by taking a second-order differentiation of the polynomial. With different filters adopted in time domain, the retrieved phases are consistent and errorless. However, after a second-order differentiation, these errors will enlarge seriously, which lead to calculated GDD that is both ambiguous and imprecise.

As mentioned above, Fourier Transform is an integral transform that converts frequency domain to time domain. The time domain actually refers to the GD domain, that is to say, every peak in the time domain represents a GD component existing in the interference field. Correspondingly, CPF is an integral transform that converts frequency domain to GDD domain [15]. The GDD can be directly obtained by applying the CPF to interference term and searching the ridge of the CPF.

Assume that $I_0(\omega)$ is the broadband source spectrum and has a Gaussian shape expressed as $\exp[-(\omega - \omega_0)^2/(2\Delta\omega^2)]$, where ω_0 is central frequency and $\Delta\omega$ is the width parameter. The differential propagation constant $\Delta\beta(\omega)$ is expanded in a Taylor series to the third order around the center frequency [6]

$$\Delta\beta(\omega) = \Delta\beta(\omega_0) + \Delta\beta^{(1)}(\omega_0) \cdot (\omega - \omega_0) + \frac{1}{2}\Delta\beta^{(2)}(\omega_0) \cdot (\omega - \omega_0)^2 + \frac{1}{6}\Delta\beta^{(3)}(\omega_0) \cdot (\omega - \omega_0)^3 \quad (3)$$

where $\Delta\beta^{(i)}(\omega_0)$ is the ith derivative of $\Delta\beta(\omega)$ with respect to ω at $\omega = \omega_0$. The relative phase can then be represented as

$$\varphi(\omega) = \left[\Delta\beta(\omega_0)l - \frac{\Delta d}{c}\omega_0\right] + \left[\Delta\beta^{(1)}(\omega_0)l - \frac{\Delta d}{c}\right](\omega - \omega_0) + \frac{1}{2}\Delta\beta^{(2)}(\omega_0)l(\omega - \omega_0)^2 + \frac{1}{6}\Delta\beta^{(3)}(\omega_0)l(\omega - \omega_0)^3. \quad (4)$$

The GDD of PMF is $\Delta\beta^{(2)}(\omega_0)l + \Delta\beta^{(3)}(\omega_0)l(\omega - \omega_0)$. Thus, the interference term is equal to a cubic phase signal with Gaussian amplitude modulation

$$I(\omega) = I_0(\omega) \cdot \exp(i\varphi(\omega)) = \exp\left[-\frac{(\omega - \omega_0)^2}{2\Delta\omega^2} + i\varphi(\omega)\right]. \quad (5)$$

The CPF of interference term $I(\omega)$ can take the following definition [15]:

$$CP(\omega, \mathrm{T}) = \int_0^{+\infty} I(\omega + \omega')I(\omega - \omega')\exp(-i\mathrm{T}\omega'^2)d\omega' \quad (6)$$

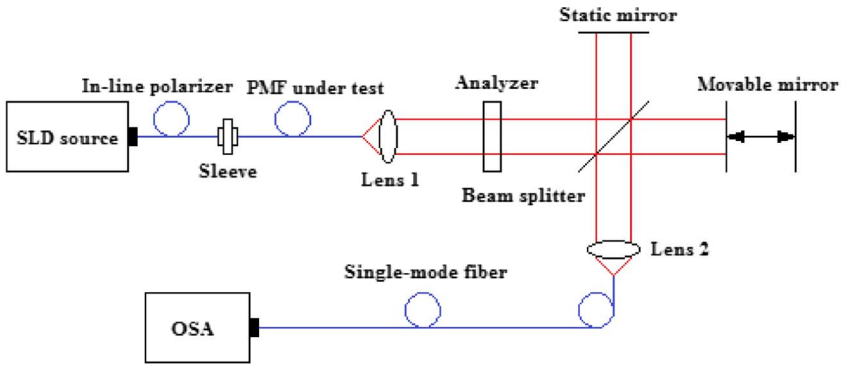

Fig. 2. The experimental setup used for obtaining the spectral interferogram.

where T is an indicator in the GDD domain, and its dimension is second^2 (s^2). Substituting (5) into (6) yields

$$CP(\omega, \mathrm{T}) = I^2(\omega)\frac{\sqrt{\pi}}{2}\left\{\frac{1}{\Delta\omega^2} - j\left[\Delta\beta^{(2)}(\omega_0)l + \Delta\beta^{(3)}(\omega_0)l(\omega-\omega_0) - \mathrm{T}\right]\right\}^{-1}. \quad (7)$$

The modulus of CPF is maximized when $\mathrm{T} = \Delta\beta^{(2)}(\omega_0)l + \Delta\beta^{(3)}(\omega_0)l(\omega-\omega_0)$, that is exactly the GDD. Therefore, the GDD with respect to ω can be directly read from the ridge of the CPF magnitude, written as

$$GDD(\omega) = \mathrm{argmax}_{\mathrm{T}}|CP(\omega, \mathrm{T})|. \quad (8)$$

In fact, CPF is not the only algorithm to directly evaluate the second-order differentiation of the signal phase without phase retrieval, but CPF naturally shows more robustness than the rival algorithms (polynomial Wigner-Ville distributions etc.) [15], this is why we adopt CPF instead of the rival algorithm.

The CDD $\Delta D(\omega)$ can then be calculated by the following [14]:

$$\Delta D(\omega) = -\frac{1}{l}\frac{\omega^2}{2\pi c} \times GDD. \quad (9)$$

Because CPF is a bilinear transform [16], CPF cannot be directly applied to the interferogram instead of the interference term. The interference term still need to be calculated by FT technique in our proposed method. However, the phase is not necessary to retrieved, and the differentiation operation is evitable.

3. Experimental Results and Discussion

Fig. 2 shows the experimental setup used for obtaining the spectral interferogram. It consists of a superluminescent diode (SLD) source with a center wavelength of 1317.4 nm and a 3-dB bandwidth of 36 nm, an in-line fiber polarizer, a PMF under test, an analyzer, a standard free space Michelson interferometer and an OSA with wavelength resolution of 0.5 nm (YOKOGAWA AQ6370C). A matching sleeve is used to connect the in-line polarizer and the PMF. Due to the polarized angular misalignment between the polarizer and the PMF, polarization coupling is caused at the input of the PMF. The analyzer is rotatable, and the rotation angle is optimized to increase the fringe visibility [17]. As the modulation period in interferogram varies along with the OPD between two modes in PMF, a movable mirror in the Michelson interferometer can be adjusted to measurement of different length PMFs [18].

In this experiment, a 395.5 m PANDA PMF was tested. Fig. 3(a) shows a recorded interferogram of the fiber normalized by maximum. Note that the interferogram was equidistantly sampled in the wavelength domain, which was from 1270 nm to 1370 nm with total sampling

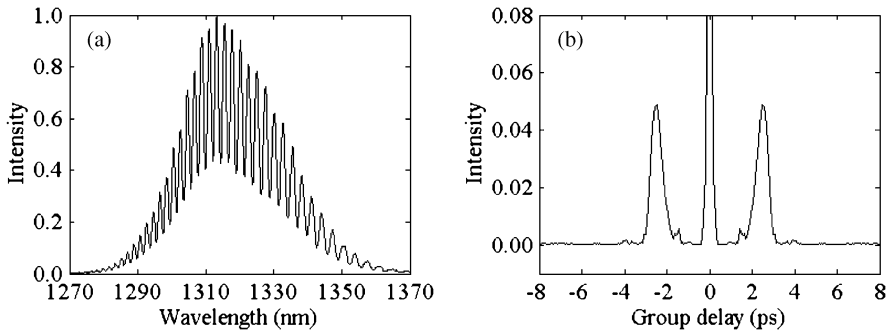

Fig. 3. (a) The spectral interferogram of PMF. (b) Fourier transform of the interferogram.

number N equal to 1001. The numerical processing started with a cubic spline interpolate algorithm to recalculate a regularly spaced interferogram in the angular frequency domain [9], from 1375.9 THz (1370 nm) to 1484.2 THz (1270 nm).

Then Fourier transform was applied to the recalculated frequency-dependent interferogram, the result is shown in Fig. 3(b). The bilateral peaks centered at ± 2.5 ps represent the two interference terms. A correct filter to extract one of the peaks should include the GD bandwidth and exclude the noise as well. As seen in Fig. 3(b), the noise spread across the whole time domain and is noticeable especially around the peak. It is difficult to find a criterion for selecting the most correct filter. Three ideal filters were adopted as examples. Filter 1 and Filter 2 are centered at the right peak at 2.5 ps with width of 1.9 ps and 3.3 ps, respectively. Filter 3 is from 0.4 ps to 29 ps. Filter 3 can be seen as only excluding the non-interference peak. 29 ps is the Nyquist limit of GD, calculated as $(2\pi)/(2\Delta\omega)$, where $\Delta\omega$ is the recalculated sampling interval. These filters are all ideal filters. For example, for Filter 1, the GD from 1.55 ps to 3.45 ps are preserved, whereas the GD from -29 ps to 1.55 ps and from 3.45 ps to 29 ps are completely excluded. This filter is realized in a simple program, where all the intensities of GD from 1.55 ps to 3.45 ps are multiplied by 1, whereas other intensities are multiplied by zero.

For each filter, an inverse Fourier transform is following to derive interference term $I(\omega_k)$ $(k = 1, 2, 3, \ldots, N)$. CPF can be calculated in the discrete form expressed as [15]

$$CP(\omega_n, \mathrm{T}) = \sum_{m=0}^{\frac{(N-1)}{2}} I(\omega_{n+m}) I(\omega_{n-m}) \exp(-i\mathrm{T}\Delta\omega^2). \tag{10}$$

At every frequency point, a nest loop program was applied to calculate the CPF with respect to T and search for the maximum of CPF magnitude. From (10), we can see that more cycles would be executed to achieve a higher resolution of GDD measurement, which will consume more time. There is a compromise between the resolution of T and the costing time. In order to reduce the number of cycles and the costing time, the maximization is implemented with a "coarse" search from -0.06 ps^2 to $+0.06$ ps^2 with resolution of 1000 fs^2, followed by a "refined" search with resolution of 25 fs^2, followed by a "re-refined" search with final resolution of 1 fs^2. The total costing time is 25 s for the total 1001 wavelength points (running in Matlab 2011b with Intel Xeon CPU E3-1225 V2 @ 3.20 GHz), whereas direct search from -0.06 ps^2 to $+0.06$ ps^2 with resolution of 1 fs^2 will take more than 10 minutes on the computer. Fig. 4 shows the CPF magnitude images from the "coarse" search for the three filters respectively. The x-axis has been converted back to wavelength domain. The measured GDD from the final "re-refined" search is superimposed as a red curve in each CPF magnitude image.

During the procedure, phase retrieval and differentiation operation are avoided. Close-view of the three GDD read from the ridges are depicted in one figure; see Fig. 5(a). As a comparison, GDD from second-order differentiation of the phases are shown in Fig. 5(b) for the three filters respectively. Because a third-order polynomial curve fitting is applied to the phase before the

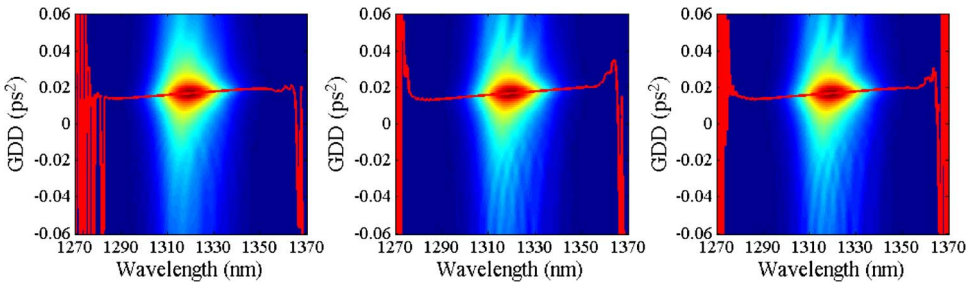

Fig. 4. The CPF magnitude images and the ridges. (From left to right: Filter 1, Filter 2, and Filter 3, respectively.)

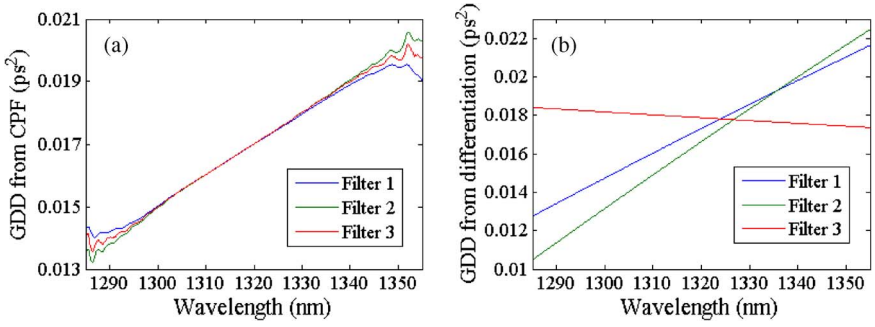

Fig. 5. (a) GDD from ridge of CPF for three filters. (b) GDD from differentiation of phases for three filters.

differentiation, the measured GDD from differentiation are linear with respect to the frequency. It can be seen GDD from ridge of CPF is more unambiguous when different filters are adopted, although slightly prone to noise out of the 3-dB bandwidth. For Filter 3, the CDD can be calculated from (9), which is illustrated in Fig. 6. Moreover, a linear fitting with respect to frequency is adjusted to the GDD from CPF. The third order dispersion (third-order differentiation of the relative phase) can be calculated as -8.97×10^{-41} s^3.

Filters centered at the interference peak with different width values are adopted to analyze the same interferogram. The measured GDD at center wavelength changes along with the width, see Fig. 7. The center wavelength GDD from CPF is almost unaltered when the width value varies from 1 ps to 4.8 ps. However the GDD from differentiation varies irregularly, it can merely be relatively accurate in the range from 2.5 ps to 4.2 ps, which has only half breadth of the range from 1 ps to 4.8 ps. This demonstrates that our proposed method can provide GDD less sensitive to the filter choice. To illustrate the versatility, another interferogram of a 168.4 m PMF is analyzed. The interference peaks are centered at $\pm$2.3 ps in the GD domain, and the measured GDD at center wavelength are also depicted in Fig. 7, with respect to filter width. As long as the filter includes most of the GD band and excludes most of the non-interference band, which is from 0.5 ps to 4.5 ps for this interferogram, our proposed method can derive more precise and unambiguous GDD than differentiation operations.

In fact, phase retrieved from the argument of the calculated interference term can be expressed as $\varphi_r(\omega) = \varphi(\omega) + E(\omega)$, where $\varphi(\omega)$ is the true spectral phase of the PMF, $E(\omega)$ is the error of the phase retrieval, which is determined by the error in the calculated interference term. $E(\omega)$ is minimized at the center wavelength and becomes higher further from the center wavelength because the signal-to-noise ratio (SNR) in the interference term is maximized at the center wavelength. A fitting polynomial of $\varphi_r(\omega)$ is expected to be as close as $\varphi(\omega)$. However, the $E(\omega)$ around the center wavelength and the $E(\omega)$ further from the center wavelength have the same influence on the fitting. Consequently, the quadratic and higher order

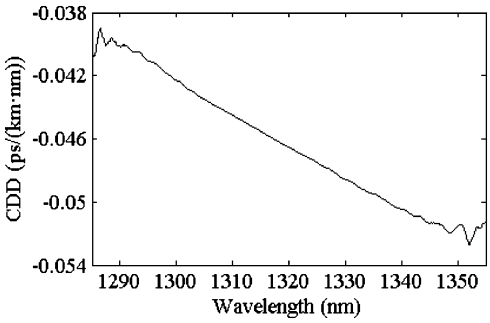

Fig. 6. Measured CDD for Filter 3.

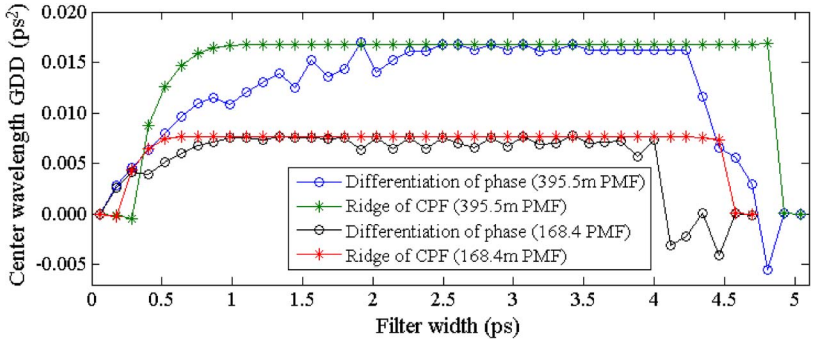

Fig. 7. Measured GDD at center wavelength with respect to filter width.

coefficients of the fitting polynomial, which are proportional to the GDD, are imprecise even around the center wavelength. In other words, the error around the center wavelength is enlarged after the fitting. As the error varies along with the filter of interference term calculation, the measured GDD from phase retrieval and differentiation is sensitive to the filter choice.

In the CPF algorithm, phase retrieval and differentiation operation can be completely avoided. From (10), we can see that the local intensity is taken into account when GDD at a certain wavelength is evaluated. The measured GDD around the center wavelength is principally impacted by the error in the interference term around the center wavelength instead of further from the center wavelength. With different filter parameters adopted, the error changes but the SNR still remains high around the center wavelength. Thus, the CPF algorithm can provide precise GDD which is less sensitive to the filter parameters, especially in the full width at half maximum (FWHM) of the spectrum (approximately from 1300 nm to 1340 nm in our experiment).

Additionally, the GDD and the CDD of the 395.5 m fiber have been measured 20 times via CPF under unchanged experimental conditions and unchanged algorithm parameters (Filter 3 is adopted). As comparison, other two algorithms are performed to process the same 20 interferograms. The first is FT technique to retrieve phase (Filter 3 is adopted), along with third-order polynomial fitting to the phase and a second-order differentiation to measure GDD [14]. The second is wavelet transform (WT) technique to directly measure GD [12] (Gabor wavelet with a shaping factor of 4 [13]), along with second-order polynomial fitting to the GD and a differentiation to measure GDD. The standard deviation (SD) of the GDD from the three algorithms is depicted in Fig. 8 (FT and WT on the left, and CPF on the right). The SD of GDD from CPF is less than 0.0002 ps^2 from 1300 nm to 1340 nm and less than 0.0001 ps^2 at center wavelength, whereas the SD of GDD from FT and WT has a minimum of about 0.001 ps^2 in the spectrum. Without phase retrieval and differentiation operation, CPF appears to be more precise than FT and WT algorithms in the measurement of GDD. This verifies the validity and superiority of the

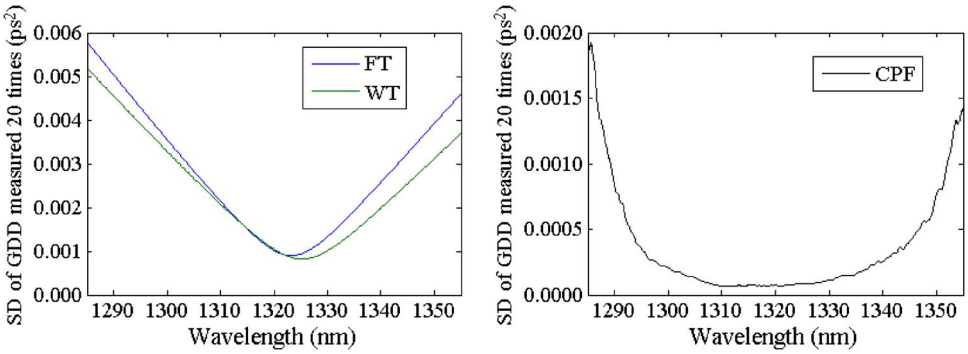

Fig. 8. SD of GDD measured 20 times (FT and WT on the left and CPF on the right).

CPF algorithm. Moreover, the SD of CDD from CPF is also less than 0.5 fs/(km · nm) around the center wavelength, which is better than a temporal method we had proposed before [19].

The processing time of the FT, WT and CPF are approximately 40 ms, 5 s and 25 s, respectively, for the total 1001 wavelength points in the spectrum. The time of FT algorithm is so less because discrete FT is applied via its fast algorithm, i.e., the fast FT (FFT). CPF seems to show no advantage in the time consuming. However, we can reduce the costing time if we need to measure the GDD of less wavelength points. For example, if we only need to measure the GDD at center wavelength, the processing time will be reduced to about 33 ms, while the time of FT and WT don't change because the phase and the GD should be calculated in the entire spectrum in order to perform the next differentiation operation.

In some application, the spectral phase is more suitable to fit as a higher-order polynomial [8], a CPF is not enough that a higher phase function (HPF) [20] needs to be employed, to ensure the precision of the GDD measurement. For complicated dispersion material such as chirped mirror [12] and multilayer mirror [21], because it is not suitable to regard the phase as a polynomial, CPF and HPF are futile to measure the GDD.

4. Conclusion

In conclusion, a PMF GDD measurement method from a spectral interferogram is proposed. The interferogram is obtained from our simple spectral interferometry system. The interference term is calculated from the interferogram by FT technique. The GDD can then be directly read from the ridge of the CPF of the interference term. The CDD can also be calculated from the GDD.

Our proposed method has merits of high resolution of 1 fs^2 with processing time of 25 s for 1001 wavelength points. If we only need to measure the GDD at center wavelength, the processing time will be reduced to about 33 ms. Unlike the previous technique, this measurement procedure can be achieved without phase retrieval and differentiation operation. Therefore, the results are insensitive to the filter. This method also shows a robust repetition with a CDD measuring deviation of 0.5 fs/(km · nm) around the center wavelength. This research is also useful in characterizations of dispersion measurement of other optical components.

References

[1] C. Peucheret, F. Lin, and R. J. S. Pedersen, "Measurement of small dispersion values in optical components," *Electron. Lett.*, vol. 35, no. 5, pp. 409–411, Mar. 1999.
[2] H. Zhang *et al.*, "Mitigation of the birefringence dispersion on the polarization coupling measurement in a long-distance high-birefringence fiber," *Meas. Sci. Technol.*, vol. 23, no. 2, Feb. 2012, Art. ID. 025203.
[3] V. Pervak *et al.*, "High-dispersive mirrors for femtosecond lasers," *Opt. Exp.*, vol. 16, no. 14, pp. 10 220–10 233, Jul. 2008.

[4] K. Goda and B. Jalali, "Dispersive Fourier transformation for fast continuous single-shot measurements," *Nat. Photon.*, vol. 7, no. 2, pp. 102–112, Feb. 2013.
[5] A. Gomez-Iglesias *et al.*, "Direct measurement of the group index of photonic crystal waveguides via Fourier transform spectral interferometry," *Appl. Phys. Lett.*, vol. 90, no. 26, Jun. 2007, Art. ID. 261107.
[6] D. A. Flavin, R. McBride, and J. D. C. Jones, "Dispersion of birefringence and differential group delay in polarization-maintaining fiber," *Opt. Lett.*, vol. 27, no. 12, pp. 1010–1012, Jun. 2002.
[7] J. Y. Lee and D. Y. Kim, "Versatile chromatic dispersion measurement of a single mode fiber using spectral white light interferometry," *Opt. Exp.*, vol. 14, no. 24, pp. 11 608–11 615, Nov. 2006.
[8] D. Reolon, M. Jacquot, I. Verrier, G. Brun, and C. Veillas, "High resolution group refractive index measurement by broadband supercontinuum interferometry and wavelet-transform analysis," *Opt. Exp.*, vol.14, no. 26, pp. 12 744–12 750, Dec. 2006.
[9] C. Dorrer, N. Belabas, J. P. Likforman, and M. Joffre, "Spectral resolution and sampling issues in Fourier-transform spectral interferometry," *J. Opt. Soc. Amer. B, Opt. Phys.*, vol. 17, no. 10, pp. 1795–1802, Oct. 2000.
[10] P. Hlubina, J. Lunacek, D. Ciprian, and R. Chlebus, "Windowed Fourier transform applied in the wavelength domain to process the spectral interference signals," *Opt. Commun.*, vol. 281, no. 9, pp. 2349–2354, May 2008.
[11] J. Bethge, C. Grebing, and G. Steinmeyer, "A fast Gabor wavelet transform for high-precision phase retrieval in spectral interferometry," *Opt. Exp.*, vol. 15, no. 22, pp. 14 313–14 321, Oct. 2007.
[12] Y. Deng *et al.*, "Direct measurement of group delay with joint time-frequency analysis of a white-light spectral interferogram," *Opt. Lett.*, vol. 33, no. 23, pp. 2855–2857, Dec. 2008.
[13] Y. Deng, W. Yang, and Z. Zhang, "Shape selection of wavelets for accurate chromatic dispersion measurement of white-light spectral interferograms," *Appl. Phys. B*, vol. 98, no. 2/3, pp. 347–351, Feb. 2010.
[14] X. Chen, H. Zhang, D. Jia, T. Liu, and Y. Zhang, "Spectral-domain measurement of chromatic dispersion difference of polarization modes in polarization-maintaining fibers," *J. Mod. Opt.*, vol. 58, no. 1, pp. 26–31, Jan. 2011.
[15] P. O'Shea, "A new technique for instantaneous frequency rate estimation," *IEEE Signal Process. Lett.*, vol. 9, no. 8, pp. 251–252, Aug. 2002.
[16] P. Wang, H. Li, I. Djurović, and B. Himed, "Integrated cubic phase function for linear FM signal analysis," *IEEE Trans. Aerosp. Electron. Syst.*, vol. 46, no. 3, pp. 963–977, Jul. 2010.
[17] W. Jing *et al.*, "Rotation angle optimization of the polarization eigenmodes for detection of weak mode coupling in birefringent waveguides," *Opt. Exp.*, vol. 10, no. 18, pp. 972–977, Sep. 2002.
[18] P. Hlubina, "Spectral-domain intermodal interference under general measurement conditions," *Opt. Commun.*, vol. 210, no. 3–6, pp. 225–232, Sep. 2002.
[19] F. Tang, X. Wang, Y. Zhang, and W. Jing, "Distributed measurement of birefringence dispersion in polarization-maintaining fibers," *Opt. Lett.*, vol. 31, no. 23, pp. 3411–3413, Dec. 2006.
[20] P. Wang, H. Li, I. Djurović, and B. Himed, "Performance of instantaneous frequency rate estimation using high-order phase function," *IEEE Trans. Signal Process.*, vol. 58, no. 4, pp. 2415–2421, Apr. 2010.
[21] P. Hlubina, J. Luňáček, and D. Ciprian, "Spectral interferometry and reflectometry used for characterization of a multilayer mirror," *Opt. Lett.*, vol. 34, no. 10, pp. 1564–1566, May 2009.